

Cytoplasmic Determinants Involved in Direct Lysosomal Sorting, Endocytosis, and Basolateral Targeting of Rat Igpl20 (lamp-I) in MDCK Cells

Stefan Höning and Walter Hunziker

Institute of Biochemistry, University of Lausanne, CH-1066 Epalinges, Switzerland

Abstract. Rat lysosomal glycoprotein 120 (Igpl20; lamp-I) is a transmembrane protein that is directly delivered from the *trans*-Golgi network (TGN) to the endosomal/lysosomal system without prior appearance on the cell surface. Its short cytosolic domain of 11 residues encodes determinants for direct lysosomal sorting, endocytosis and, in polarized cells, basolateral targeting. We now characterize the structural requirements in the cytosolic domain required for sorting of Igpl20 into the different pathways. Our results show that the cytoplasmic tail is sufficient to mediate direct

transport from the *trans*-Golgi network (TGN) to lysosomes and that a G7-Y8-X-X-I11 motif is crucial for this sorting event. While G7 is only critical for direct lysosomal sorting in the TGN, Y8 and I11 are equally important for lysosomal sorting, endocytosis, and basolateral targeting. Thus, a small motif of five amino acids in the cytoplasmic tail of Igpl20 can be recognized by the sorting machinery at several cellular locations and direct the protein into a variety of intracellular pathways.

LYSOSOMES contain a family of highly glycosylated transmembrane proteins (lamps) which, based on deduced amino acid sequence, can be divided into three groups, lamp-I, lamp-II, and lamp-III (for a review see Fukuda, 1991). Common features of these proteins are the significant degree of homology in overall sequence and structure, containing a highly glycosylated luminal domain, a single transmembrane anchor, and a short, highly conserved cytoplasmic tail. Although lamps have been proposed to play a role in maintaining lysosomal integrity (Kornfeld and Mellman, 1989), their actual function remains unclear.

An issue of interest and controversy has been the pathway taken by lamps after leaving the Golgi complex. One possibility is that newly synthesized lamps are directly delivered from the Golgi complex to endosomes/lysosomes without prior appearance on the cell surface. Based on kinetic studies, rat Igpl20 (lamp-I) has been suggested to follow the direct route in normal rat kidney cells (Green et al., 1987). A similar conclusion was reached by analyzing Chinese hamster ovary and MDCK cells transfected with wild-type and mutant Igpl20 (Harter and Mellman, 1992; Hunziker et al., 1991). Direct transport was further postulated for lamp-I based on cell fractionation studies in 3T3 cells (D'Souza and August, 1986). In the case of direct transport, it has been suggested that lamps may follow the same route taken by lysosomal enzymes bound to the cation-independent man-

nose 6-phosphate receptor (Kornfeld and Mellman, 1989), although direct evidence supporting this notion is lacking.

Alternatively, lamps could be first delivered to the cell surface and reach the endosomal/lysosomal system following endocytosis. Several reports have proposed an obligatory passage for different members of the lamp-I and lamp-II families through the plasma membrane en route to lysosomes. These include avian LEP100 in chicken fibroblasts and mouse L cells (Lippincott-Schwartz and Fambrough, 1987; Mathews et al., 1992), rat lamp107 (identical to rat Igpl20) in rat hepatocytes (Furuno et al., 1989a, b), and human lamp-I in human leukemia cells (Mane et al., 1989). In contrast to transfected rat Igpl20 (Hunziker et al., 1991), an endogenous canine lamp-II (AC17 antigen) has been proposed to reach lysosomes indirectly via the basolateral surface in canine kidney-derived MDCK cells (Nabi et al., 1991). Finally, the few lysosomal membrane glycoproteins studied that do not belong to the lamp family appear to reach lysosomes either following endocytosis from the cell surface (lysosomal acid phosphatase) (Braun et al., 1989), or directly from the TGN (rat lamp-II) (Vega et al., 1991).

It is to date unclear whether all lamps are delivered via the direct or indirect route, via both pathways, or whether the pathway taken depends on the individual lamp protein. Most likely, the observed discrepancies are due to different experimental parameters such as expression levels or cell types. Irrespective of whether lamps reach endosomes/lysosomes directly or indirectly, mutations in their short conserved cytoplasmic tail severely affect their correct sorting, indicating an involvement of specific signals (Williams and

Address all correspondence to W. Hunziker, Institute of Biochemistry, University of Lausanne, CH. des Boveresses 155, CH-1066 Epalinges, Switzerland. Tel.: 41-21-692-5737. Fax: 41-21-692-5705.

Fukuda, 1990; Hunziker et al., 1991; Harter and Mellman, 1992; Guarnieri et al., 1993). Although several studies have analyzed the role of a subset of lamp tail amino acids, a comprehensive analysis of the importance of all individual residues is lacking. In most instances, the effect of a particular mutation was only analyzed for one or two of the three possible sorting events. In addition, in many studies large fractions of wild-type lamp were present on the cell surface and an effect on Golgi sorting could have been masked by protein reaching lysosomes via the endocytic route.

Work to date has indicated a role for G7, Y8, and I11 in lysosomal sorting, whereas H5, A6, Q9, and T10 appear to be unimportant (Williams and Fukuda, 1990; Hunziker et al., 1991; Harter and Mellman, 1992; Guarnieri et al., 1993). However, in the study analyzing H5 and A6, wild-type lamp-I was also delivered to the plasma membrane and a possible role of these residues in direct Golgi sorting may have gone unnoticed since the mutants could also have reached lysosomes via endocytosis (Williams and Fukuda, 1990). Similarly, only the steady-state distribution of mutants affecting Q9, T10, and I11 was analyzed (Guarnieri et al., 1993), and residues critical for Golgi sorting would have gone undetected if the corresponding mutant reached lysosomes by rapid endocytosis from the cell surface. Y8 was found to be required for endocytosis and substitution of H5, A6, and G7 had no effect (Williams and Fukuda, 1990; Hunziker et al., 1991; Harter and Mellman, 1992). Finally, with respect to basolateral sorting in polarized cells, only the role of G7 and Y8 has been analyzed and Y8, but not G7, was shown to be important (Hunziker et al., 1991).

In the present study we used alanine scan mutagenesis to determine the functional importance of all cytoplasmic tail residues in direct Golgi sorting, endocytosis and basolateral targeting of Igpl20. The different tail mutants were constructed in Igpl20 or were fused to the luminal and transmembrane domains of the murine IgG FcRII-B2 receptor (Igpl20-FcR). To analyze endocytosis and basolateral sorting of mutants that were normally directly sorted from the Golgi to lysosomes (and thus did not appear on the plasma membrane), we took advantage of the observation that increased expression levels result in mistargeting of the corresponding constructs to the plasma membrane (Harter and Mellman, 1992).

Our results show that the cytoplasmic domain of Igpl20 is not only necessary but sufficient for correct intracellular transport. Y8, and I11 are critical for direct lysosomal sorting, endocytosis and basolateral targeting, whereas G7 is only involved in direct transport from the Golgi to lysosomes. Thus, Igpl20 encodes a small sorting motif capable of directing transport into a variety of intracellular pathways.

Materials and Methods

Construction of Igpl20 Tail Mutants and FcRII-B2 Ectodomain-Igpl20 Tail Chimera

To mutagenize the cytoplasmic Igpl20 domain, a unique AflII site was introduced after the transmembrane domain by PCR. Introduction of the AflII site resulted in a RIL substitution present in all constructs (see Fig. 1). This modified Igpl20 cDNA was then cloned into the expression vector pCB6 (Hunziker et al., 1991) and used as template for the subsequent PCR reactions. Sense primers covering the AflII site in the modified Igpl20 were combined with the different mutagenic antisense primers encoding the

Igpl20 tail and carrying an XbaI site in the noncoding region. PCR fragments encoding the mutated cytoplasmic domain sequences were cut with AflII/XbaI and used to replace the Igpl20 wild-type tail. To generate Igpl20-FcR, PCR products encoding wild-type and mutant Igpl20 tails were appended in frame to the ectoplasmic and transmembrane domains of an FcRII-B2 construct carrying a unique AflII site following the transmembrane domain (Matter et al., 1992) (kindly provided by K. Matter, Yale University). The sequence of the primers is available upon request. All fragments synthesized by PCR were verified by dideoxy sequencing.

Generation of MDCK Cells Stably Expressing Igpl20 and Igpl20-FcR Constructs

MDCK cells were stably transfected as described (Hunziker and Mellman, 1989). Clones expressing Igpl20 or Igpl20-FcR were screened by immunofluorescence. MDCK cells were cultured on plastic or on permeable polycarbonate filters (Transwell™; Costar Corp., Cambridge, MA) as detailed (Hunziker and Mellman, 1989). To increase expression levels, transfected cells were incubated for 12 h in growth media supplemented with 10 mM butyrate (Matter et al., 1992).

Metabolic Labeling and Immunoprecipitation

Cells were metabolically labeled overnight with 10 μ Ci/ml cysteine/methionine (35 S-EXPRESS; New England Nuclear, Boston, MA) and chased for 1 h at 37°C in the presence of a 1:100 dilution of anti-Igpl20 serum. After cooling cells on ice for 30 min, they were washed three times with PBS, lysed in 1% Triton X-100, and postnuclear supernatants were incubated with protein A-Sepharose to precipitate Igpl20 that had appeared on the cell surface and thus had bound anti-Igpl20 antibodies. Fresh anti-Igpl20 serum was added to the supernatant of the first precipitation to immunoprecipitate total labeled Igpl20. Samples were analyzed by SDS-PAGE (7.5% acrylamide), dried gels exposed to X-ray film, and band intensity quantified by densitometry. To analyze the cell surface appearance of newly synthesized Igpl20, cells were starved in DMEM lacking cysteine and methionine for 30 min and pulse labeled for 15 min with 0.5 mCi/ml [35 S]cysteine/methionine. After washing, cells were chased for different periods of time in complete medium containing a 1:100 dilution of anti-Igpl20 serum. Cells were cooled on ice, washed, and processed for immunoprecipitation as described above. The polarized distribution of Igpl20, as well as the insertion of newly synthesized protein into the apical or basolateral surfaces of MDCK cells grown on Transwell™ units was determined as described (Hunziker et al., 1991). Experiments involving Igpl20-FcR chimera were carried out as described above, except that an anti-FcRII serum was used instead of the anti-Igpl20 antibody. Polyclonal anti-Igpl20 and anti-FcR sera were kindly provided by I. Mellman (Yale University, New Haven, CT).

Endocytosis Assays

Endocytosis of Igpl20 or Igpl20-FcR was analyzed on living cells by immunofluorescence (see below). Endocytosis rates were obtained by measuring the uptake of iodinated Fab fragments of the anti FcRII monoclonal antibody 2.4G2 (Unkeless, 1979) by cells expressing Igpl20-FcR constructs. After binding 125 I-2.4G2 Fab fragments (1 μ g/ml) on ice for 60 min, unbound Fab fragments were removed by washing with ice-cold PBS. The cells were incubated at 37°C in DMEM, 0.5% BSA for different periods of time to allow for endocytosis to occur and then returned on ice. Fab fragments still present on the surface were removed by washing with acid (DMEM, 0.5% BSA, pH 2.2.) and ligand released into the media, present on the cell surface or intracellular (acid resistant) was determined and plotted as the percent of total initially bound radioactivity (1×10^{-6} cpm).

Immunofluorescence

Cells grown on glass coverslips were fixed in methanol for 2 min at -20°C, nonspecific binding sites were blocked with 10% goat serum, and cells were incubated with either a polyclonal or monoclonal (Ly1C6) anti-rat Igpl20 (Igpl20-expressing cells), or with a polyclonal or monoclonal (2.4G2) anti-FcRII antibody (Igpl20-FcR-expressing cells). Endogenous MDCK lamp-II was detected using the monoclonal antibody AC17 (Nabi et al., 1991) (kindly provided by A. LeBivic, University of Marseilles). Primary antibodies were detected using 1:100 dilutions of the corresponding labeled secondary antibodies. Coverslips were mounted in Mowiol and viewed with a Zeiss Axiophot microscope. Pictures were taken on Kodak T-Max 400 film, using identical conditions for exposure, development, and printing. To

detect endocytosis of surface Igpl20 or Igpl20-FcR, living cells were incubated for 60 min at 37°C with a 1:100 dilution of polyclonal anti-Igpl20 or FcRII antisera, or with 1 µg/ml of monoclonal Ly1C6 or 2.4G2 antibody in DMEM, 0.5% BSA. After cooling on ice, cells were washed, fixed, and processed for immunofluorescence as outlined above.

Results

The Cytoplasmic Domain of Igpl20 Is Sufficient for Correct Sorting to Lysosomes

We first determined whether the cytosolic domain of Igpl20 was not only required but sufficient to mediate correct sorting from the TGN to lysosomes. For this purpose, MDCK cells were generated that stably expressed a chimeric protein consisting of the IgG FcRII-B2 ectodomain and transmembrane region fused to the cytoplasmic tail of Igpl20 (Igpl20-FcR; see Fig. 1). To analyze whether the chimeric Igpl20-FcR was correctly sorted, we first used immunofluorescence to compare its steady-state distribution to that of wild-type Igpl20. Cells expressing either wild-type Igpl20 or Igpl20-FcR were fixed, permeabilized, and stained with an antibody to Igpl20 or FcRII, respectively. As shown in Fig. 2 *F*, the Igpl20-FcR chimera localized to a vesicular perinuclear compartment that was indistinguishable from that carrying Igpl20 (Fig. 2 *A*). Neither wild-type Igpl20 nor the chimeric protein could be detected on the cell surface at steady-state. However, since Igpl20 or Igpl20-FcR could escape detection on the plasma membrane if, following surface appearance, they reached lysosomes by rapid endocytosis, we incubated living cells for 60 min at 37°C in the presence of an antiserum to Igpl20 or FcR, respectively. As shown in Fig. 3, *A* and *F*, no antibody was internalized at 37°C by cells expressing either Igpl20 or Igpl20-FcR, suggesting that the chimeric protein did not reach lysosomes via rapid endocytosis from the cell surface. That this assay was in principle able to detect Igpl20 or Igpl20-FcR delivered via the cell surface was evident from the fact that butyrate-treated cells overexpressing the corresponding proteins (see below) did internalize antibodies (Fig. 3, *A'* and *F'*). Finally, the vesicular structures containing Igpl20 or the chimera represented bona fide lysosomes as was confirmed by the fact that staining for Igpl20 and Igpl20-FcR colocalized at least partially with that for an endogenous MDCK lamp-II protein (Fig. 2, *A*, *A'* and *F*, *F'*), revealed by the monoclonal antibody AC17 (Nabi et al., 1991).

These results indicate that the cytoplasmic tail of Igpl20 is not only required but also sufficient for direct sorting from the TGN to lysosomes.

G7, Y8, and I11 Are Critical for Direct Delivery from the Golgi to Lysosomes

We next analyzed the importance of the 11 individual amino acids in the cytoplasmic tail of Igpl20 in direct sorting from the Golgi to lysosomes. For this purpose, alanine scan mutagenesis was used to substitute single residues in the cytosolic tail as outlined in Fig. 1. In addition, chimeric FcR were constructed carrying the mutated Igpl20 cytoplasmic domains. MDCK cell lines stably expressing the different constructs were identified by immunofluorescence and characterized.

To obtain a first indication as to the importance of the different cytoplasmic residues, the steady-state distribution

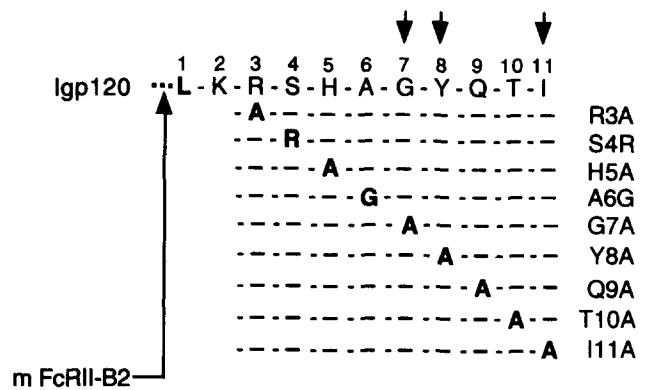


Figure 1. Amino acid sequences of the cytoplasmic domains of wild-type and mutant Igpl20 and Igpl20-FcR. Sequences are shown in the single-letter code and the residues substituting amino acids in the wild-type sequence are in bold. All constructs contained an R1L substitution at position 1 resulting from the introduction of a unique restriction site (see Materials and Methods). Residues are numbered from left to right, with position 1 corresponding to the presumed first amino acid of the cytoplasmic domain.

of the Igpl20 and Igpl20-FcR constructs was analyzed. Cells were fixed, permeabilized, and stained with an antibody to Igpl20 or FcR, respectively. The same perinuclear vesicular staining pattern observed for wild-type Igpl20 (Fig. 2 *A*) was observed for all mutants except those carrying substitutions of Y8 or I11 (not shown, Fig. 2, *C* and *D*). Both Y8A and I11A were exclusively detected on the cell surface and no intracellular labeling was observed. Similar staining patterns were obtained for the corresponding Igpl20-FcR tail mutants (not shown), suggesting that they behaved like their Igpl20 counterparts.

The exclusive vesicular staining observed for all Igpl20 mutants except those affecting Y8 and I11 suggested that they were directly delivered from the TGN to lysosomes, as has been proposed for the wild-type protein. However, it was conceivable that mutant protein was not detected on the cell surface at steady-state, perhaps reflecting low amounts due to rapid endocytosis. Therefore, we next incubated living cells in the presence of anti-Igpl20 antibody for 60 min at 37°C. Under these conditions, antibody can bind to and be internalized by Igpl20 even if it only transiently appears on the cell surface, resulting in the intracellular accumulation of antibody (Hunziker et al., 1991; Harter and Mellman, 1992). After washing and fixing the cells, they were permeabilized and anti-Igpl20 that had been internalized was visualized by immunofluorescence using a labeled secondary reagent.

As shown in Fig. 3, no anti-Igpl20 was detected either on the cell surface or intracellularly in cells expressing wild-type Igpl20 (Fig. 3 *A*). Anti-Igpl20 antibody was also not detected in cells expressing any of the mutants except for G7A, Y8A, and I11A (not shown, see below), suggesting that like wild-type Igpl20 these mutants were delivered to lysosomes without prior appearance on the cell surface. In contrast, in cells expressing the G7A mutant, the anti-Igpl20 was detected in typical lysosomal structures, showing that G7A was delivered to the cell surface where it bound and internalized anti-Igpl20 antibody (Fig. 3 *B*). Cells expressing Y8A and I11A, on the other hand, although exhibiting a bright surface

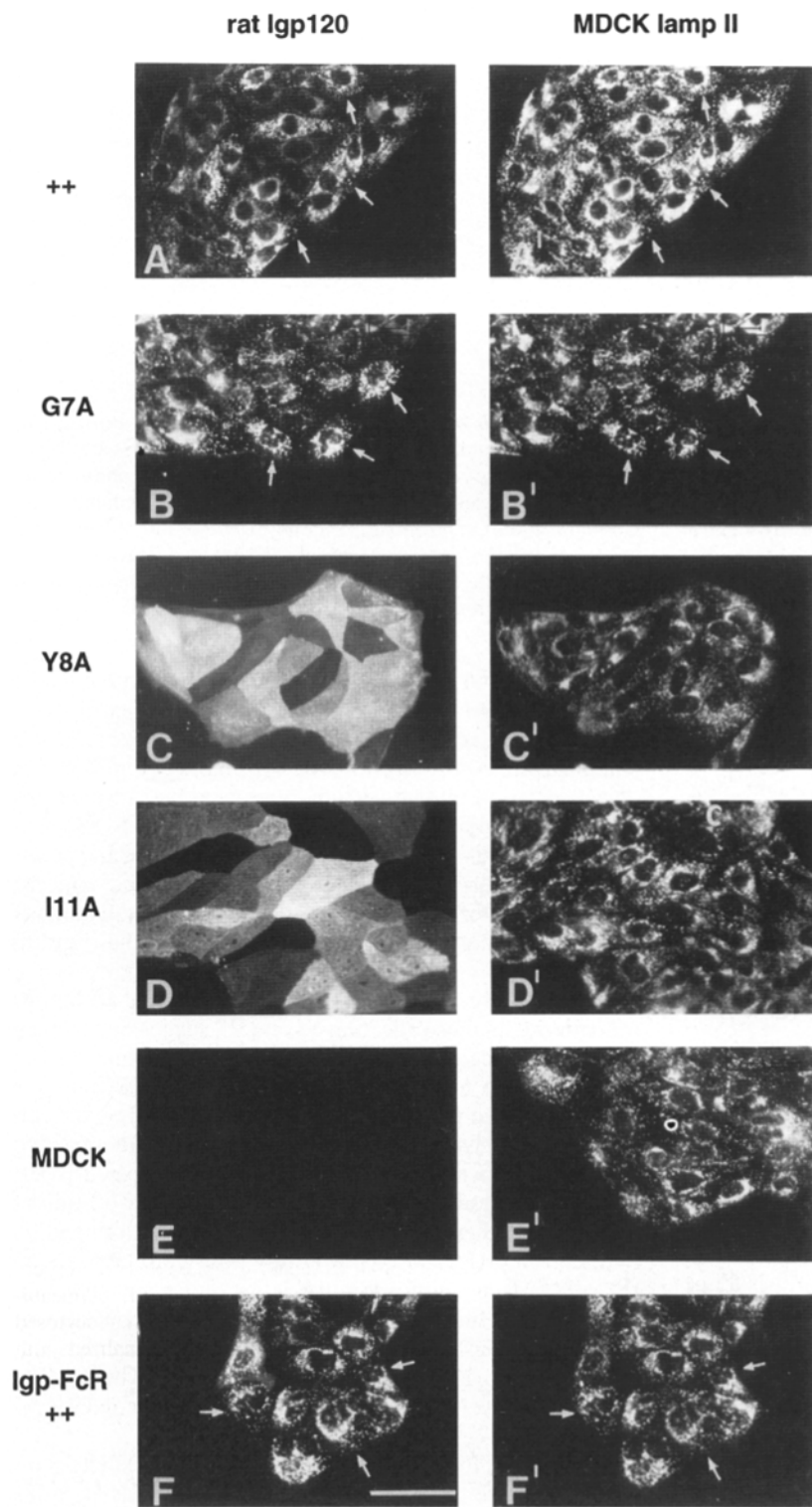


Figure 2. Colocalization of wild-type and mutant Igpl20 and Igpl20-FcR with endogenous MDCK lamp-II. Non-transfected and MDCK cells transfected with wild-type or mutant rat Igpl20 or Igpl20-FcR were fixed and processed for immunofluorescence. Igpl20 and Igpl20-FcR (*left*) were stained with polyclonal antisera to Igpl20 or FcRII, respectively. Endogenous MDCK lamp-II was stained with monoclonal antibody AC17 (*right*). DTAF-conjugated goat anti-rabbit IgG and Texas Red-labeled goat anti-mouse IgG second antibodies were used. Arrows indicate selected regions of colocalization. A and A': Igpl20; B and B': Igpl20 G7A; C and C': Igpl20 Y8A; D and D': Igpl20 I11A; E and E': MDCK control cells; F and F': Igpl20-FcR. Bar, 60 μ m.

labeling, lacked the vesicular staining, indicating that they did not internalize the antibody (Fig. 3, C and D). Similar results were obtained when these experiments were performed with cells expressing the corresponding Igpl20-FcR tail mutants (not shown, see below).

The above results were confirmed biochemically by ana-

lyzing the cell surface delivery of newly synthesized wild-type or mutant Igpl20. Cells were pulse labeled for 15 min with [35 S]cysteine/methionine and then chased for different periods of time. Anti-Igpl20 was present throughout the chase to allow the detection of Igpl20 transiently exposed on the plasma membrane. After washing and lysing the cells,

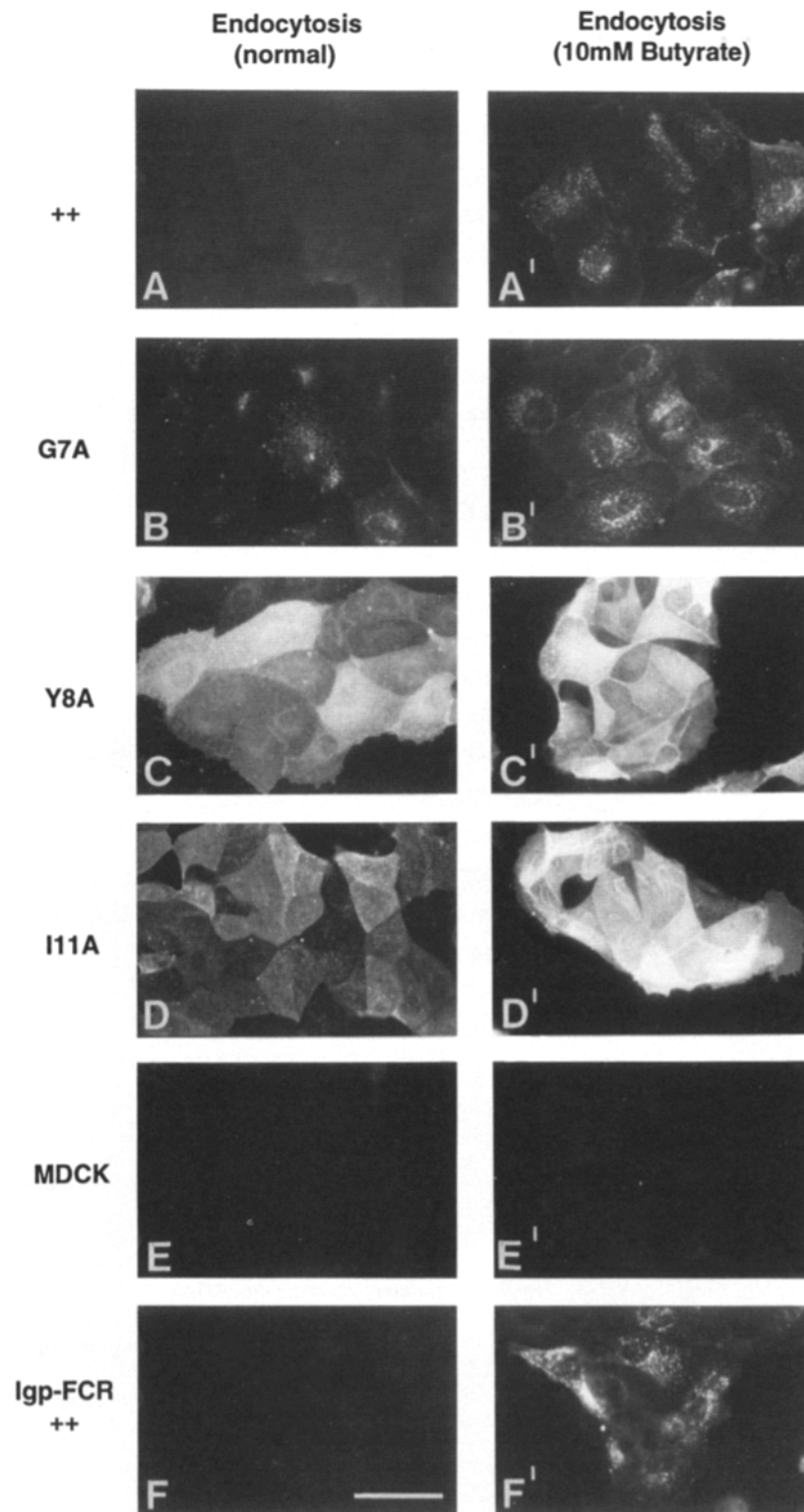


Figure 3. Surface distribution and endocytosis of Igpl20 in transfected MDCK cells. Non-transfected and MDCK cells transfected with wild-type and mutant rat Igpl20 or Igpl20-FcR were incubated for 60 min at 37°C in the presence of an antibody to Igpl20 or FcR, respectively. The cells were then fixed, permeabilized, and surface bound or endocytosed anti-Igpl20 or anti-FcR was visualized with Texas Red-labeled anti-mouse IgG (*left*). The same experiment was also performed with butyrate-treated cells overexpressing the different proteins (*right*). A and A', Igpl20; B and B', Igpl20 G7A; C and C', Igpl20 Y8A; D and D', Igpl20 II1A; E and E', MDCK control cells; F and F', Igpl20-FcR. Bar, 60 μ m.

Igpl20 that had reached the cell surface—and therefore had bound anti-Igpl20—was isolated by absorption to protein A-Sepharose.

As shown in Fig. 4, less than 4% of the total labeled wild-type Igpl20 could be precipitated following a 120-min chase. Except for G7A, Y8A, and II1A, similar low levels of surface

appearance were observed for the remaining mutants (not shown). In contrast, 20–45% of newly synthesized G7A, Y8A or II1A were recovered, indicating that a significant fraction of these mutants reached the plasma membrane.

Taken together, these results are consistent with direct delivery of Igpl20 from the TGN to lysosomes. Further-

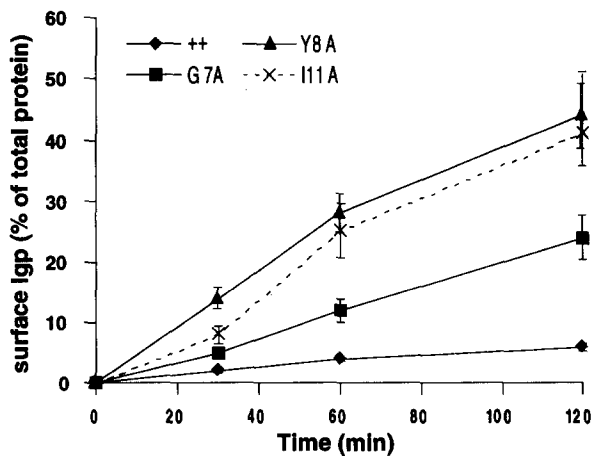


Figure 4. Plasma membrane delivery of newly synthesized Igpl20. Cells expressing wild-type or mutant Igpl20 were pulse labeled with [³⁵S]cysteine/methionine for 15 min and chased for the indicated periods of time at 37°C in the presence of an anti-Igpl20 serum. After cell lysis, labeled Igpl20 that had bound antibody after exposure on the cell surface was absorbed to immobilized protein A. Total Igpl20 was isolated following the addition of fresh antiserum. Immunoprecipitates were analyzed by SDS-PAGE and autoradiography and two independent experiments were quantitated by densitometry. Error bars show the range of variation of the values.

more, they show that G7A, Y8A, and I11A are critically involved in mediating direct sorting of Igpl20 from the Golgi to lysosomes.

Overexpression of Wild-type and Mutant Igpl20 Results in Surface Delivery

It has previously been shown that overexpression of Igpl20 in CHO cells results in surface delivery of transfected Igpl20 and endogenous lamp-II (Harter and Mellman, 1992). We therefore determined whether overexpression of the different Igpl20 mutants in MDCK cells also led to their delivery to the plasma membrane, since this would allow us to determine the structural requirements in the cytoplasmic domain important for endocytosis and basolateral sorting.

For this purpose, we took advantage of the fact that butyrate can increase expression of proteins under control of the CMV promoter in the expression vector pCB6 (Matter et al., 1992). Cells were metabolically labeled in the presence or absence of butyrate for 12 h and total labeled Igpl20 was determined by immunoprecipitation. As shown in Fig. 5 A, comparable levels of Igpl20 were synthesized by non-butyrate-treated cells expressing the different constructs (*hatched bars*). In cells that had been incubated in the presence of butyrate, however, a three- to eightfold stimulation of Igpl20 synthesis was observed (*filled bars*).

We next determined the fraction of the different Igpl20 constructs present on the cell surface in the absence or presence of butyrate. Metabolically labeled cells were incubated with anti-Igpl20 antibodies for 60 min at 37°C and the fraction of labeled Igpl20 that had been exposed to the cell surface during this period was determined. As shown in Fig. 5 B, 15–30% of the G7A, Y8A, or I11A protein became exposed on the cell surface in control cells and butyrate-treatment did not significantly affect the fraction of these mutants that reached the surface. In contrast, while less than 2%

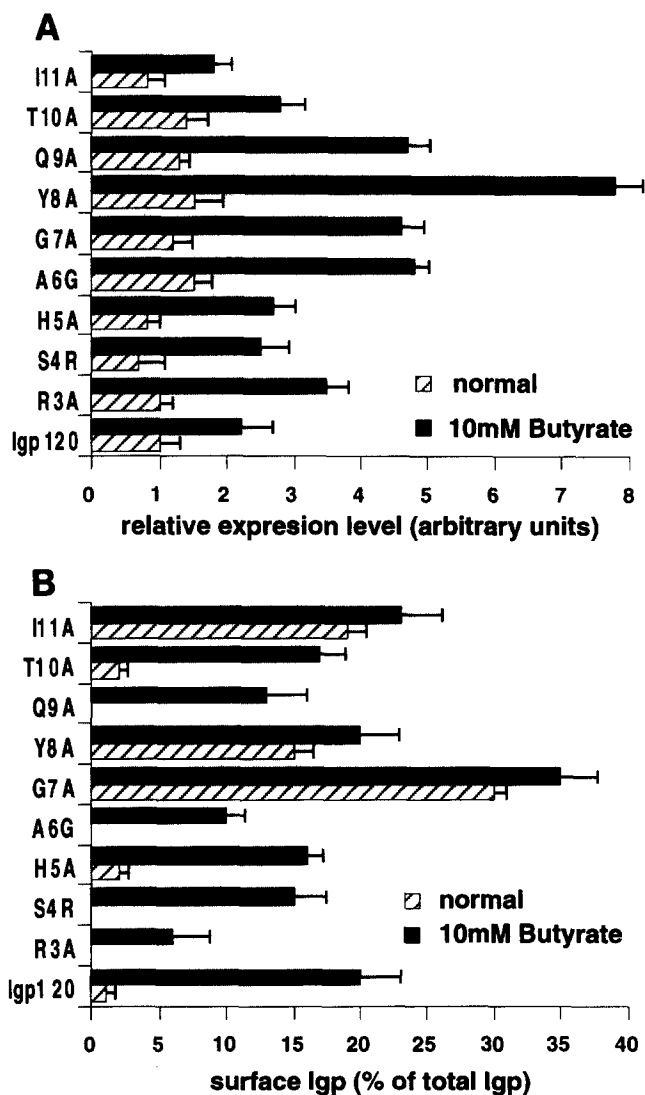


Figure 5. Expression levels and surface appearance of Igpl20 in butyrate treated cells. Cells expressing wild-type or mutant Igpl20 were labeled overnight with [³⁵S]cysteine/methionine in the presence or absence of 10 mM butyrate. After washing, the cells were incubated for one hour at 37°C in the presence of anti-Igpl20 serum. After cell lysis, labeled Igpl20 that had bound antibody after exposure on the cell surface was absorbed to immobilized protein A. Total Igpl20 was isolated following the addition of fresh antiserum. Immunoprecipitates were analyzed by SDS-PAGE and autoradiography and three independent experiments were quantitated by densitometry and averaged. (A) Total labeled Igpl20. (B) The fraction of total labeled Igpl20 that had reached the plasma membrane. Error bars show the range of variation of the values.

of the protein was exposed on the surface in cells expressing the remaining mutants or wild-type Igpl20, butyrate treatment led to the appearance of 6–20% of the Igpl20 on the plasma membrane. Thus, butyrate only increased the surface expression of wild-type or Igpl20 constructs that were not already present on the plasma membrane under normal conditions.

These observations were confirmed by immunofluorescence experiments. Control or butyrate-treated cells were incubated for 60 min at 37°C in the presence of anti-Igpl20 an-

tibody. Cells were then washed, fixed, and permeabilized, and the anti-Igpl20 antibody was visualized by immunofluorescence. While only cells expressing G7A, Y8A, or I11A were stained in the absence of butyrate (Fig. 3, B–D), anti-Igpl20 antibody could be detected in all cells expressing either wild-type Igpl20 (Fig. 3 A') or any of the mutants following butyrate treatment (not shown). Except for cells expressing the Y8A and I11A mutants (Fig. 3, C' and D'), a vesicular staining pattern was observed, suggesting that antibody bound on the surface was internalized by cells overexpressing the corresponding Igpl20 constructs (not shown, see below).

Taken together, these results show that increasing Igpl20 expression levels leads to the cell surface appearance of wild-type and mutant Igpl20 normally not present on the plasma membrane.

Y8 and I11 Are Critical for Endocytosis

The immunofluorescence experiments described above suggested that only the substitution of Y8 and I11 affected the ability of Igpl20 present on the cell surface to endocytose. We next confirmed these results quantitatively and also analyzed the kinetics of internalization for the different Igpl20 tail mutants. Since the behavior of the Igpl20-FcR constructs was indistinguishable from that of the corresponding Igpl20 mutants, the following experiments were carried out with cells expressing the Igpl20-FcR chimera. This allowed us to take advantage of the well characterized Fab fragments of the 2.4G2 anti-FcR monoclonal antibody to study endocytosis (Mellman et al., 1984; Hunziker and Mellman, 1989; Hunziker et al., 1990). Cells expressing the different Igpl20-FcR constructs were treated with butyrate to induce surface transport even of mutants normally not delivered to the plasma membrane. After binding radioiodinated 2.4G2 Fab fragments to the cells on ice, non-bound ligand was removed by washing and cells were warmed to 37°C to allow for endocytosis to occur. After different periods of time, the cells were returned on ice and the fraction of ligand that had been internalized was determined.

As shown in Fig. 6, A and B, except for Y8A and I11A, all chimeric proteins rapidly and efficiently endocytosed Fab fragments, with 40–50% of the bound ligand being intracellular after 60 min. Although the final extent of internalization was similar for all constructs, endocytosis by wild-type Igpl20-FcR and G7A occurred with slightly faster kinetics as compared to the remaining mutants. The final extent of internalization by the G7A mutant was slightly higher than that of wild-type Igpl20-FcR, possibly reflecting more efficient delivery of G7A from early endosomes to internal compartments, or more efficient recycling of Igpl20-FcR to the cell surface. Cells expressing either Y8A or I11A, on the other hand, internalized less than 15% of the prebound Fab.

In conclusion, these results confirm the immunofluorescence results described above and show that Y8 and I11 play equally important roles for the rapid and efficient endocytosis of Igpl20.

Y8 and I11 Are Critical for Basolateral Sorting in Polarized MDCK Cells

Several proteins delivered to the basolateral plasma membrane in epithelial cells carry collinear but distinct tyrosine-dependent basolateral sorting and endocytosis signals

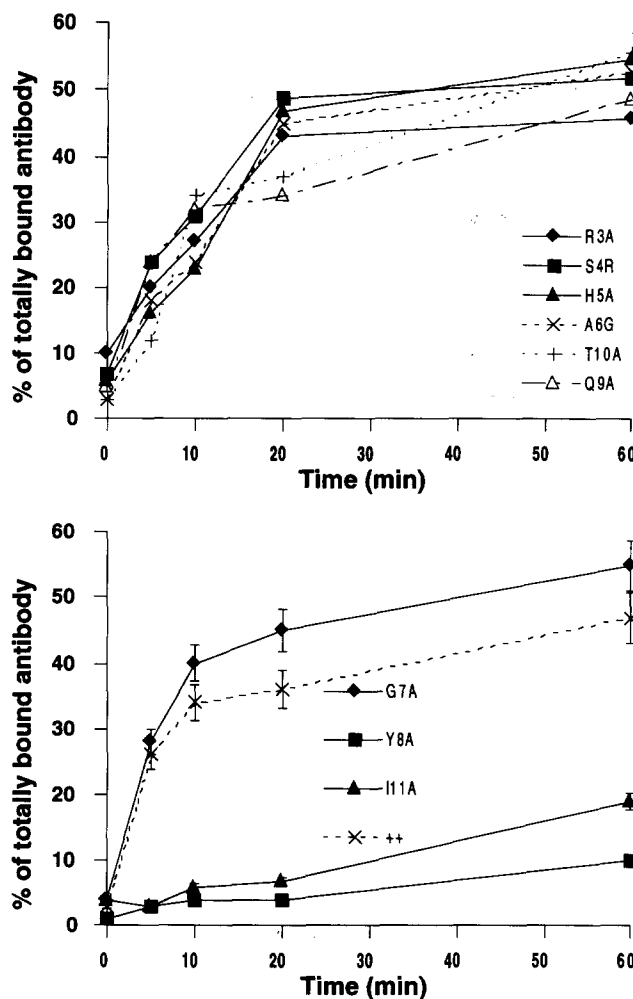


Figure 6. Kinetics of 2.4G2 internalization by cells overexpressing wild-type and mutant Igpl20-FcR. Iodinated Fab fragments of the monoclonal anti-FcR antibody 2.4G2 were bound on ice to MDCK cells expressing the different Igpl20-FcR constructs. After washing, cells were transferred to 37°C to allow internalization of Fab fragments to occur. Cells were returned on ice and endocytosis the amount of acid resistant radioactivity associated with the cells was determined. Values are expressed as % total initially bound cpm ($10\text{--}50 \times 10^4$) and represent the mean of two independent experiments. Error bars show the range of variation of the values.

(reviewed in Rodriguez-Boulan and Zurzolo, 1993). This close correlation between basolateral sorting and endocytosis function has also been observed for Igpl20: while the endocytosis-competent G7A mutant has been shown to be delivered basolaterally, the endocytosis-deficient Y8C construct was found on the apical domain (Hunziker et al., 1991). It was therefore of interest to determine the effect of substitutions affecting the remaining cytoplasmic tail residues on the polarized transport of Igpl20. For this purpose, MDCK cells expressing the different Igpl20 or Igpl20-FcR mutants were grown on Transwell™ filter units to obtain polarized cell monolayers.

First, the equilibrium distribution of the different constructs on the apical or basolateral surface was determined by quantitating the binding of iodinated 2.4G2 Fab fragments from the two compartments on ice. As shown in Fig. 7 A, the distribution of the G7A and Y8A Igpl20-FcR chi-

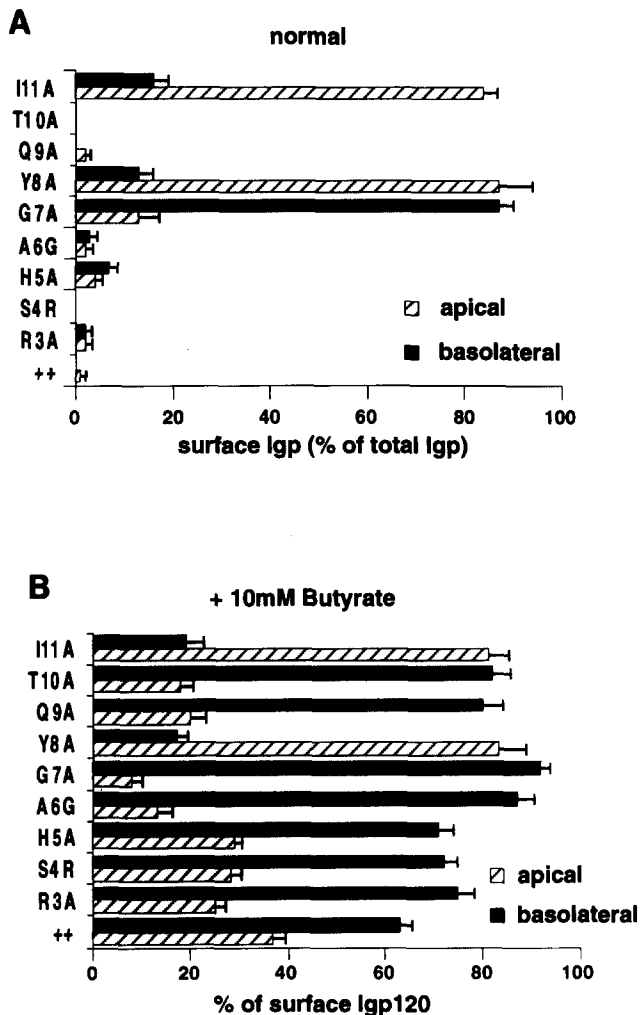


Figure 7. Polarized cell surface distribution of mutant Igpl20-FcR in polarized MDCK cells. Cells expressing the different Igpl20-FcR constructs were grown on Transwell™ units. Non-butyrate-treated (A) or butyrate-treated (B) cells were incubated on ice with radiolabeled 2.4G2 Fab fragments added either from the apical or the basolateral compartment on ice. Unbound antibody was removed by washing, filters were cut out and bound radioactivity determined. Values for nonspecific binding, determined in the presence of a 100-fold excess of unlabeled 2.4G2 IgG, were subtracted and represented 10–15% of the total binding ($2-6 \times 10^4$ cpm). Experiments were carried out in duplicate and error bars show the range of variation of the values.

mera confirmed previous results obtained with the corresponding Igpl20 mutants (Hunziker et al., 1991): while >75% of G7A was present on the basolateral surface, >80% of Y8A localized apically. Interestingly, also I11A was found almost exclusively on the apical cell surface. As already observed for cells grown on plastic, neither wild-type Igpl20-FcR nor any other mutant besides G7A, Y8A, and I11A could be detected on the plasma membrane. In order to analyze the polarized transport of these constructs, cells were treated with butyrate to obtain surface delivery of the overexpressed proteins. As shown in Fig. 7 B, the polarized distribution of G7A, Y8A, and I11A in butyrate-treated cells was comparable to the one obtained in control cells. The remaining mutants (R3A, S4R, H5A, A6G, Q9A, and T10A), as well as

wild-type Igpl20-FcR, were mostly found on the basolateral surface, although the degree of basolateral polarity varied from 65–85% for the different constructs. Similar results were obtained using the corresponding Igpl20 constructs and surface immunoprecipitation (not shown).

Since the steady-state distribution of a given protein on the apical or basolateral membrane is the result of both biosynthetic delivery and transcytosis (for a review see Hunziker and Mellman, 1991), and since low levels of Igpl20 transcytose in a basolateral to apical direction (Matter et al., 1993), we next analyzed whether the distribution of the constructs reflected the direct polarized delivery of newly synthesized protein from the TGN to the respective plasma membrane surface. For this purpose, filter-grown cells expressing the different Igpl20 constructs were pulse-labeled with [³⁵S]methionine/cysteine and labeled proteins chased to the cell surface for different periods of time (Hunziker et al., 1991). To detect Igpl20 arriving either at the apical or basolateral cell surface, anti-Igpl20 serum was included into one or the other compartment during the chase. Cells were lysed and labeled Igpl20 bound to antibody was isolated by absorption to immobilized protein A (Hunziker et al., 1991).

As shown in Fig. 8 and consistent with published results (Hunziker et al., 1991), pulse-labeled G7A and Y8A were directly inserted into the basolateral or apical domain, respectively. Similar to Y8A, also newly synthesized I11A was directly delivered to the apical surface. As observed above, no significant levels of wild-type Igpl20 or any of the remaining mutants (R3A, S4R, H5A, A6G, Q9A, and T10A) could be detected on the cell surface. The polarized transport of these mutants was therefore analyzed in cells treated with butyrate. Polarized cell surface insertion of G7A, Y8A and I11A was identical to that observed in non-butyrate-treated cells. Transport of newly synthesized R3A, S4R, H5A, A6G, Q9A, and T10A and wild-type Igpl20 to the plasma membrane occurred in a polarized fashion and these constructs were almost exclusively inserted into the basolateral domain.

In conclusion, these experiments reveal equally important roles for Y8 and I11 in the basolateral sorting determinant encoded by the cytoplasmic tail of Igpl20.

Discussion

Sorting Determinants in Igpl20

The goal of the present study was to analyze in detail the structural determinants involved in lysosomal sorting, endocytosis and basolateral targeting of Igpl20. Our results show that the Igpl20 tail is not only required, but also sufficient for direct segregation from the TGN to lysosomes. G7, Y8, and I11 were critical for direct delivery to lysosomes, whereas Y8 and I11 played equally important roles in endocytosis and polarized targeting. None of the remaining residues was essential for directing Igpl20 into the different pathways.

The finding that chimera between the FcRII-B2 extracellular and transmembrane domains and the Igpl20 cytoplasmic tail were delivered to lysosomes following the same pathway as wild-type Igpl20 indicates that the 11 residues short tail is sufficient for mediating correct sorting of Igpl20 from the TGN to lysosomes. Previously, chimera between plasma

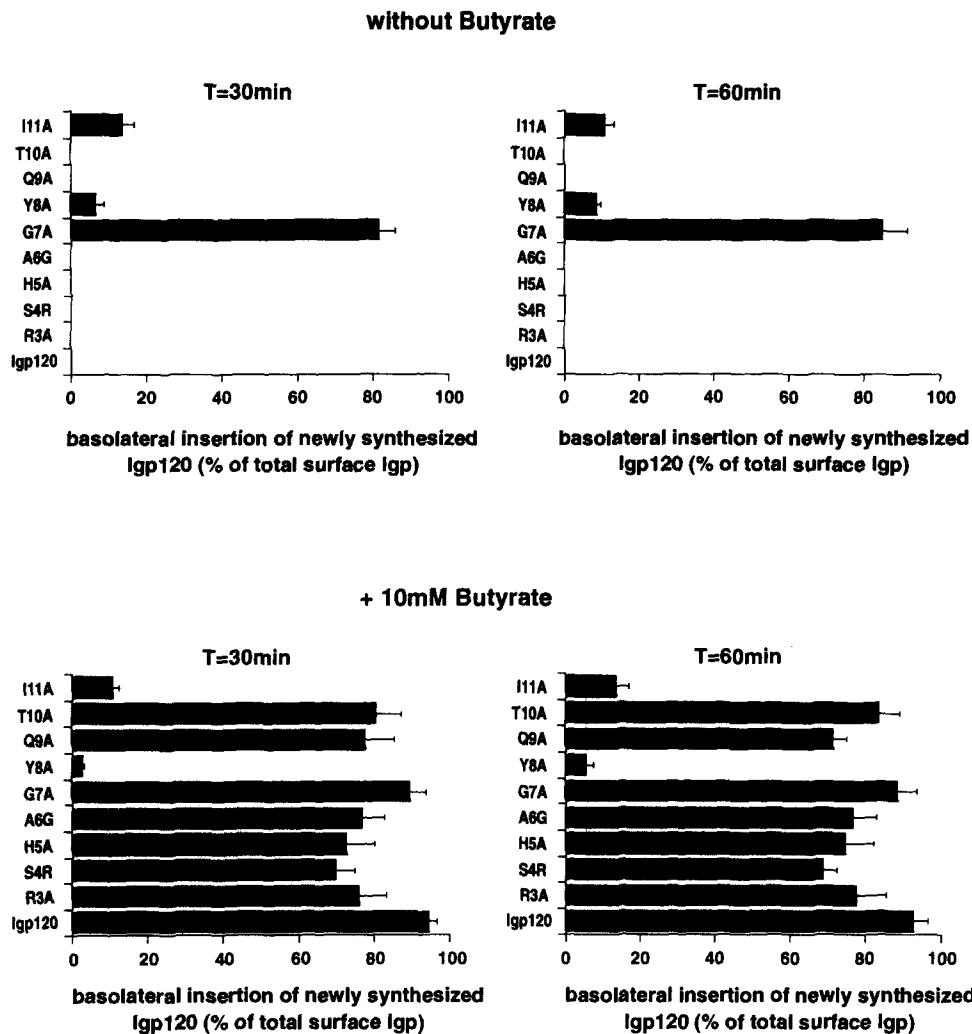


Figure 8. Polarized cell surface insertion of newly synthesized mutant Igp120. MDCK cells expressing the Igp120 constructs were grown on Transwell™ units in the presence (+10 mM butyrate) or absence (without butyrate) of butyrate. After pulse-labeling with [³⁵S]methionine/cysteine for 15 min, cells were chased for 30 (T = 30 min) or 60 min (T = 60 min) in the presence of anti-Igp120 serum added to the apical or basolateral chamber. Cells were then washed on ice, lysed, and labeled Igp120 that had appeared on the cell surface (and thus bound anti-Igp120) was precipitated with immobilized protein A. Total Igp120 was precipitated with additional antiserum. Samples were analyzed by SDS-PAGE and autoradiography. Following quantitation by densitometry, surface protein was normalized to total labeled Igp120. The relative fraction of total surface protein inserted into the basolateral domain is shown for the different constructs. Error bars show the range of variation of the values.

membrane proteins and the tail of either LEP100 (Mathews et al., 1992) or human-lamp-I (Williams and Fukuda, 1990) have been shown to reach lysosomes. However, since those studies postulated an indirect route to lysosomes and a large fraction of wild-type LEP100 or lamp-I was delivered to lysosomes via the cell surface and subsequent endocytosis, they could not distinguish whether the cytoplasmic tail of lamp-I was able to mediate direct sorting at the TGN or only endocytosis. Similarly, at steady-state a chimera of a plasma membrane protein and the murine lamp-I tail was found to display a lysosomal distribution by immunofluorescence (Guarnieri et al., 1993). However, also that work did not analyze whether the chimera reached lysosomes via the direct or indirect route. Therefore, the findings of those studies could not a priori be extrapolated for Igp120. Our experiments now conclusively show that the Igp120 (lamp-I) tail can by itself mediate direct transport from the TGN to lysosomes. Transport of Igp120-FcR to endosomes/lysosomes occurred directly from the TGN and did not involve the plasma membrane since no intracellular accumulation of antibody added to living cells was detected (see below).

The short cytoplasmic domains of lamp proteins have been implicated in at least three different sorting events: direct delivery from the TGN to lysosomes, endocytosis, and basolateral targeting in polarized cells. Although the role of sev-

eral of the cytoplasmic residues in one or the other intracellular pathway has been analyzed in the past, no definitive conclusions have been possible for several reasons. First, in many of the studies, a large fraction of the wild type lamp-I was delivered to lysosomes via the cell surface and it was therefore impossible to conclude whether substitution of a residue affected Golgi sorting, endocytosis, or both. For example, while G7 was required for Golgi-sorting in cells where no wild-type Igp120 was routed through the plasma membrane (Hunziker et al., 1991; Harter and Mellman, 1992), this role for G7 went unnoticed in cells expressing significant levels of wild-type protein on the plasma membrane (Williams and Fukuda, 1990). Similarly, studies analyzing the equilibrium distribution of lamp-I mutants affecting Q9, T10, and I11 failed to address the possibility that the mutants may be delivered to lysosomes via the cell surface (Guarnieri et al., 1993). This problem is again apparent for the G7A mutant which, by immunofluorescence, displays a typical lysosomal distribution with little if any protein present on the surface at equilibrium (see Fig. 2 B). Nevertheless, a significant fraction of G7A reaches lysosomes via the plasma membrane and endocytosis. With respect to basolateral sorting, finally, only the involvement of G7 and Y8 has been analyzed (Hunziker et al., 1991).

In the present study we now conclusively show that G7, Y8,

and I11 are required for direct delivery of Igpl20 from the TGN to lysosomes. In the G7-Y8-X-X-I11 motif, I11 has been suggested to possibly tolerate substitutions by other bulky aliphatic residues such as leucine and phenylalanine (Guarnieri et al., 1993). Interestingly, although lysosomal acid phosphatase carries a similar motif (G-Y-X-X-V), it is predominantly delivered to lysosomes via the cell surface. One difference between the two proteins is the location of the signal within the protein and it remains to be determined whether a COOH-terminal exposure of the sorting motif as found in Igpl20 improves recognition in the TGN. These sequence requirements in Igpl20 differ from the di-leucine/leucine-isoleucine-based motifs found in other proteins directly delivered from the TGN to endosomes/lysosomes, such as the mannose 6-phosphate receptor (Johnson and Kornfeld, 1992) and limp-II (Ogata and Fukuda, 1994; Sandoval et al., 1994). Transport of the mannose 6-phosphate receptor is thought to occur via TGN-derived clathrin-coated vesicles (Marquardt et al., 1987) and the cytoplasmic domain of the receptor binds to Golgi-derived AP-1 adaptor complexes (Glickman et al., 1989). Whether lamp proteins are delivered to endosomes/lysosomes in the same clathrin-coated vesicles as the mannose 6-phosphate receptor, or whether they utilize a different type of carriers, remains to be determined.

G7, while required for direct sorting of Igpl20 from the TGN to lysosomes, was not important for basolateral sorting or endocytosis. Nevertheless, the latter two events still depended on the presence of Y8 and I11 and substitution of either residue completely abolished endocytosis and basolateral sorting. A bulky aliphatic amino acid two positions downstream of the critical tyrosine as found in the Igpl20 tail often occurs in internalization signals, although a number of determinants have a polar or charged residue in this place. Lysosomal acid phosphatase, for example, carries a valine at the corresponding position and NMR studies have indicated that this region may form a β -type turn structure in solution (Eberle et al., 1991), a critical feature of many endocytosis signals (reviewed in Vaux, 1992). Whether also the Y-X-X-I sequence in Igpl20 forms a β -turn remains to be established, but the Y-X-X-I motif closely resembles a classical coated pit internalization signal. Interestingly, while the rates of endocytosis of the wild type and the G8A chimera were very similar, substitution of either R3, S4, H5, A6, Q9, or T10 resulted in slightly but significantly slower initial rates, suggesting that these residues may make minor contributions to an optimal internalization determinant.

Similar to the clustering of endocytic receptors into clathrin-coated pits, polarized sorting of proteins to the basolateral surface of epithelial cells requires the presence of distinct cytoplasmic tail determinants (reviewed by Mellman et al., 1993; Hunziker and Mellman, 1991; Mostov et al., 1992; Rodriguez-Boulan and Zurzolo, 1993). These signals appear to belong to two classes: those that are colinear with the endocytosis information (Brewer and Roth, 1991; Hunziker et al., 1991; LeBivic et al., 1991; Matter et al., 1992; Geffen et al., 1993; Thomas et al., 1993), and those that reside on a separate region (Casanova et al., 1991; Matter et al., 1992; Okamoto et al., 1992; Yakode et al., 1992; Dargemont et al., 1993). For both classes, tyrosine-dependent and -independent signals have been described. Where basolateral signals overlapping with the coated pit determinant

have been analyzed in more detail, the two were found to be distinct (Hunziker et al., 1991; Matter et al., 1992; Prill et al., 1993), although a di-leucine-based motif may be responsible for both functions in the IgG FcR2-B2 (Hunziker and Fumey, 1994).

The results obtained for Igpl20 are particularly interesting with respect to this apparent relationship between basolateral sorting and endocytosis signals, because both sorting functions were absolutely dependent on the presence of Y8 and I11. Although the substitution mutants that did not reach the cell surface under normal expression levels were delivered to the basolateral domain in butyrate treated cells, they were less well polarized at steady-state. Several possibilities could explain this reduced basolateral polarity at equilibrium. First, since R3A, S4R, H5A, A6G, Q9A, and T10A are capable of endocytosis, the mutants could reach the apical domain by transcytosis. Indeed, low levels of basolateral to apical transcytosis have been observed for overexpressed wild-type Igpl20 (Matter et al., 1993). Second, R3, S4, H5, A6, Q9, and T10 could make small contributions to the sorting signal, similar to their minor importance for an optimal endocytosis determinant. Third, the Igpl20 tail could encode a "weak" basolateral sorting signal similar to the membrane proximal determinant in the LDL-R (Matter et al., 1992). In this case, overexpression of the protein could lead to the saturation of the sorting machinery and missorting to the apical domain. Against this latter possibility argues the observation that basolateral delivery of the respective mutants from the TGN occurred with a higher degree of polarity than reflected in their steady-state localization. In addition, since alanine scan mutagenesis only examines the ability of a certain position to tolerate this particular substitution, it is not possible to determine the exact contribution of other residues to the two sorting functions. As found for lysosomal acid phosphatase (Prill et al., 1993), substitution of Y8 by other aromatic residues such as phenylalanine may affect endocytosis but not basolateral sorting. Nevertheless, the structural requirements for endocytosis and basolateral sorting of Igpl20 are very similar (if not identical), with Y8 and I11 representing the key residues.

Interestingly, a similar Y-X-X-I motif has recently been shown to be responsible for basolateral sorting of vesicular stomatitis virus G protein (Thomas and Roth, 1994). In G protein, the Y-X-X-I signal required a minimal distance of at least five residues from the transmembrane domain, similar to the distance of this element in Igpl20. In contrast to Igpl20, however, the Y-X-X-I motif did not appear to confer endocytic activity to G protein.

Little is known about the secondary structure of basolateral sorting signals. Based on NMR studies, the tyrosine-independent determinant in the pIgR tail was proposed to form a β -type turn containing a critical valine at position 660 (Aroeti et al., 1993). However, until the structure of other basolateral signals has been resolved, it remains to be seen whether the formation of a β -turn is a common structural feature of these determinants.

Routing of lamp Proteins to Lysosomes

One issue under debate is whether lamp proteins are directly transported from the TGN to endosomes/lysosomes, or whether they are first delivered to the plasma membrane and

then reach lysosomes via the endocytic route. Although lamps are capable of undergoing rapid endocytosis from the plasma membrane, even where a fraction of the protein was routed through the cell surface (Williams and Fukuda, 1990), the predominant pathway was proposed to be direct from the Golgi to lysosomes (Carlsson and Fukuda, 1992). Delivery of lamp proteins to the cell surface could well reflect the saturation of the sorting machinery in the Golgi complex due to overexpression. Indeed, in Chinese hamster ovary cells, increasing expression levels of rat Igpl20 has been shown to result in surface delivery of transfected and endogenous lamp-II (Harter and Mellman, 1992). Similarly, we observed that inducing expression of Igpl20 by treating cells with butyrate resulted in cell surface transport of wild-type and mutant Igps normally directly targeted to lysosomes. Surface delivery of mutants already transported to the plasma membrane at low expression levels (i.e., G7A, Y8A, or I11A), was not increased in butyrate stimulated cells, consistent with the idea that overexpression saturates a specific sorting step in the TGN that does not affect proteins lacking the signals required for recognition by the sorting machinery. However, we can not rule out other effects of butyrate, perhaps on direct Golgi sorting. Alternatively, following delivery from the TGN to an endosomal compartment, some lamp mutants could be less efficiently transported to lysosomes and, as a consequence, recycle to the plasma membrane from an endosomal compartment. However, since less than 10% of 2.4G2 Fab internalized by any of the Igpl20-FcR constructs was recycled (data not shown), it is unlikely that surface transport of wild-type or mutant Igpl20 occurs from endosomes.

Although it was not our primary aim to analyze the exact route taken by Igpl20, our results support the idea of a direct delivery from the TGN to endosomes/lysosomes without prior appearance on the cell surface. The non-butyrate-stimulated cells in our study expressed similar levels of the different Igpl20 mutants and wild-type protein, yet only G7A, Y8A, and I11A were detected on the cell surface, showing that surface transport of G7A, Y8A, and I11A was not due to overexpression. G7A, and certainly Y8A and I11A, may have bound antibody present in the media more efficiently if they were exposed on the cell surface longer than the wild-type protein or the other mutants. However, the kinetics of endocytosis for the wild-type and the G7A chimera were identical, suggesting that the ability to detect the G7A mutant, but not wild-type Igpl20, on the cell surface, did not reflect better antibody binding by G7A due to a longer residence time on the plasma membrane. In fact, also mutants with slightly slower endocytosis rates than G7A or wild type Igpl20 (i.e., R3A, S4R, H5A, A6G, Q9A, or T10A) could not be detected on the cell surface. Intracellular accumulation of antibody present in the media by G7A but not by the wild-type protein could also have reflected that G7A, but not wild-type Igpl20, preferentially recycled back to the cell surface following internalization. However, less than 10% of 2.4G2 Fab fragments preinternalized by Igpl20-FcR or any of the mutants was recycled back to the cell surface (not shown), indicating that multiple rounds of internalization and recycling by the G7A mutant was not responsible for the observed uptake of antibody. In conclusion, our observations strongly argue for direct sorting of Igpl20 from the TGN

to lysosomes and for a role of G7, Y8, and I11 in this sorting event.

Further characterization of the pathway taken by Igpl20 will now require to determine whether or not lamp proteins are included into the same TGN-derived clathrin-coated vesicles as the mannose 6-phosphate receptor, or whether they follow a different route. In addition, it will be important to identify the cytosolic sorting machinery involved in lysosomal and basolateral sorting of lamp proteins.

We thank C. Furney for excellent technical assistance, C. Kamel and T. Simmen for their support, advice and for critically reading the manuscript, and I. Mellman and A. LeBivic for kindly providing antibodies.

This work was supported by a grant and a Career Development (START) Award from the Swiss National Science Foundation to W. Hunziker.

Received for publication 18 August 1994 and in revised form 17 October 1994.

References

- Aroeti, B., P. A. Rosen, I. D. Kuntz, F. E. Cohen, and K. E. Mostov. 1993. Mutational and secondary structural analysis of the basolateral sorting signal of the polymeric immunoglobulin receptor. *J. Cell Biol.* 123:1149-1160.
- Braun, M., A. Waheed, and K. von Figura. 1989. Lysosomal acid phosphatase is transported to lysosomes via the cell surface. *EMBO (Eur. Mol. Biol. Organ.) J.* 8:3633-3640.
- Brewer, C. B., and M. G. Roth. 1991. A single amino acid change in the cytoplasmic domain alters the polarized delivery of influenza virus hemagglutinin. *J. Cell Biol.* 114:413-421.
- Carlsson, S. R., and M. Fukuda. 1992. The lysosomal membrane glycoprotein lamp-1 is transported to lysosomes by two alternative pathways. *Arch. Biochem. Biophys.* 296:630-639.
- Casanova, J. E., G. Apodaca, and K. E. Mostov. 1991. An autonomous signal for basolateral sorting in the cytoplasmic domain of the polymeric immunoglobulin receptor. *Cell.* 66:65-75.
- D'Souza, M. P., and J. T. August. 1986. A kinetic analysis of biosynthesis and localization of a lysosome-associated membrane glycoprotein. *Arch. Biochem. Biophys.* 249:522-532.
- Dargemont, C., A. LeBivic, S. Rothenberger, B. Iacopetta, and L. C. Kuhn. 1993. The internalization signal and the phosphorylation site of transferrin receptor are distinct from the main basolateral sorting information. *EMBO (Eur. Mol. Biol. Organ.) J.* 12:1713-1721.
- Eberle, W., C. Sander, W. Klaus, B. Schmidt, K. von Figura, and C. Peters. 1991. The essential tyrosine of the internalization signal in lysosomal acid phosphatase is part of a β turn. *Cell.* 67:1203-1209.
- Fukuda, M. 1991. Lysosomal membrane glycoproteins. Structure, biosynthesis, and intracellular trafficking. *J. Biol. Chem.* 266:21327-21330.
- Furuno, K., T. Ishikawa, K. Akasaki, S. Yano, Y. Tanaka, Y. Yamaguchi, H. Tsuji, M. Himeno, and K. Kato. 1989a. Morphological localization of a major lysosomal membrane glycoprotein in the endocytic membrane system. *J. Biochem.* 106:708-716.
- Furuno, K., S. Yano, K. Akasaki, Y. Tanaka, Y. Yamaguchi, H. Tsuji, M. Himeno, and K. Kato. 1989b. Biochemical analysis of the movement of a major lysosomal membrane glycoprotein in the endocytic membrane system. *J. Biochem.* 106:717-722.
- Geffen, I., C. Fuhrer, B. Leitinger, M. Weiss, K. Huggel, G. Griffiths, and M. Spiess. 1993. Related signals for endocytosis and basolateral sorting of the asialoglycoprotein receptor. *J. Biol. Chem.* 268:20772-20777.
- Glickman, J. A., E. Conibear, and B. M. F. Pearse. 1989. Specificity of binding of clathrin adaptors to signals on the mannose-6-phosphate/insulin-like growth factor II receptor. *EMBO (Eur. Mol. Biol. Organ.) J.* 8:1041-1047.
- Green, S. A., K.-P. Zimmer, G. Griffiths, and I. Mellman. 1987. Kinetics of intracellular transport and sorting of lysosomal membrane and plasma membrane proteins. *J. Cell Biol.* 105:1227-1240.
- Guarnieri, F. G., L. M. Arterburn, M. B. Penno, Y. Cha, and J. T. August. 1993. The motif Tyr-X-X-hydrophobic residue mediates lysosomal membrane targeting of lysosome-associated membrane protein-1. *J. Biol. Chem.* 268:1941-1946.
- Harter, C., and I. Mellman. 1992. Transport of the lysosomal membrane glycoprotein Igpl20 (Igp-A) to lysosomes does not require appearance on the plasma membrane. *J. Cell Biol.* 117:311-325.
- Hunziker, W., and I. Mellman. 1989. Expression of macrophage-lymphocyte Fc receptors in MDCK cells: polarity and transcytosis differ for isoforms with or without coated pit localization domains. *J. Cell Biol.* 109:3291-3302.
- Hunziker, W. and J. Hellman. 1991. Relationships between sorting in the exocytic and endocytic pathways of MDCK cells. *Semin. Cell Biol.* 2:397-470.

- Hunziker, W., and C. Fumey. 1994. A di-leucine motif mediates endocytosis and basolateral sorting of macrophage IgG Fc receptors in MDCK cells. *EMBO (Eur. Mol. Biol. Organ.) J.* 13:2963-2969.
- Hunziker, W., P. Male, and I. Mellman. 1990. Differential microtubule requirements for transcytosis in MDCK cells. *EMBO (Eur. Mol. Biol. Organ.) J.* 9:3515-3525.
- Hunziker, W., C. Harter, K. Matter, and I. Mellman. 1991. Basolateral sorting in MDCK cells requires a distinct cytoplasmic domain determinant. *Cell.* 66:907-920.
- Johnson, K. F., and S. Kornfeld. 1992. A His-Leu-Leu sequence near the carboxyl terminus of the cytoplasmic domain of the cation-dependent mannose 6-phosphate receptor is necessary for the lysosomal enzyme sorting function. *J. Biol. Chem.* 267:17110-17115.
- Kornfeld, S., and I. Mellman. 1989. The biogenesis of lysosomes. *Annu. Rev. Cell Biol.* 5:483-525.
- LeBivic, A., Y. Sambuy, A. Patzak, N. Patil, M. Chao, and E. Rodriguez-Boulan. 1991. An internal deletion in the cytoplasmic tail reverses the apical localization of human NGF receptor in transfected MDCK cells. *J. Cell Biol.* 115:607-618.
- Lippincott-Schwartz, J., and D. M. Fambrough. 1987. Cycling of the integral membrane glycoprotein, LEP100, between plasma membrane and lysosomes: kinetic and morphological analysis. *Cell.* 49:669-677.
- Mane, S. M., L. Marzella, D. F. Bainton, V. K. Holt, Y. Cha, J. E. Hildreth, and J. T. August. 1989. Purification and characterization of human lysosomal membrane glycoproteins. *Arch. Biochem. Biophys.* 268:360-378.
- Marquardt, T., T. Braulke, A. Hasilik, and K. von Figura. 1987. Association of the precursor of cathepsin D with coated membranes: kinetics and carbohydrate processing. *Eur. J. Biochem.* 168:37-42.
- Mathews, P. M., J. B. Martinie, and D. M. Fambrough. 1992. The pathway and targeting signal for delivery of the integral membrane glycoprotein LEP100 to lysosomes. *J. Cell Biol.* 118:1027-1040.
- Matter, K., W. Hunziker, and I. Mellman. 1992. Basolateral sorting of LDL receptor in MDCK cells—the cytoplasmic domain contains 2 tyrosine-dependent targeting determinants. *Cell.* 71:741-753.
- Matter, K., J. A. Whitney, E. M. Yamamoto, and I. Mellman. 1993. Common signals control low density lipoprotein receptor sorting in endosomes and the Golgi complex of MDCK cells. *Cell.* 74:1053-1064.
- Mellman, I., H. Plutner, and P. Ukkonen. 1984. Internalization and rapid recycling of macrophage Fc receptors tagged with monovalent antireceptor antibody: possible role of a prelysosomal compartment. *J. Cell Biol.* 98:1163-1169.
- Mellman, J., E. Yamamoto, J. A. Whitney, M. Kim, W. Hunziker, and K. Matter. 1993. Molecular sorting in polarized and non-polarized cells—common problems, common solutions. *J. Cell Sci. Suppl.* 17:1-7.
- Mostov, K., G. Apodaca, B. Aroeti, and C. Okamoto. 1992. Plasma membrane protein sorting in polarized epithelial cells. *J. Cell Biol.* 116:577-583.
- Nabi, I. R., A. LeBivic, D. Fambrough, and E. Rodriguez-Boulan. 1991. An endogenous MDCK lysosomal membrane glycoprotein is targeted basolaterally before delivery to lysosomes. *J. Cell Biol.* 115:1573-1584.
- Ogata, S., and M. Fukuda. 1994. Lysosomal targeting of limp II membrane glycoprotein requires a novel Leu-Ile motif at a particular position in its cytoplasmic tail. *J. Biol. Chem.* 269:5210-5217.
- Okamoto, C. T., S.-P. Shia, C. Bird, K. E. Mostov, and M. G. Roth. 1992. The cytoplasmic tail of the polymeric immunoglobulin receptor contains two internalization signals that are distinct from its basolateral sorting signal. *J. Biol. Chem.* 267:9925-9932.
- Prill, V., L. Lehmann, K. von Figura, and C. Peters. 1993. The cytoplasmic tail of lysosomal acid phosphatase contains overlapping but distinct signals for basolateral sorting and rapid internalization in polarized MDCK cells. *EMBO (Eur. Mol. Biol. Organ.) J.* 12:2181-2193.
- Rodriguez-Boulan, E., and C. Zurzolo. 1993. Polarity signals in epithelial cells. *J. Cell Sci. Suppl.* 17:9-12.
- Sandoval, I. V., J. J. Arredondo, J. Alcalde, A. G. Noriega, J. Vandekerckhove, M. A. Jimenez, and M. Rico. 1994. The residues Leu(Ile)(475)-Ile(Leu,Val,Aal)(476), contained in the extended carboxyl cytoplasmic tail, are critical for targeting of the resident lysosomal membrane protein limp II to lysosomes. *J. Biol. Chem.* 269:6622-6631.
- Thomas, D. C., and M. G. Roth. 1994. The basolateral targeting signal in the cytoplasmic domain of glycoprotein g from vesicular stomatitis virus resembles a variety of intracellular targeting motifs related by primary sequence but having diverse targeting activities. *J. Biol. Chem.* 269:15732-15739.
- Thomas, D. C., C. B. Brewer, and M. G. Roth. 1993. Vesicular stomatitis virus glycoprotein contains a dominant cytoplasmic basolateral sorting signal critically dependent upon a tyrosine. *J. Biol. Chem.* 268:3313-3320.
- Unkeless, J. C. 1979. Characterization of a monoclonal antibody directed against mouse macrophage and lymphocyte Fc receptors. *J. Exp. Med.* 150:580-596.
- Vaux, D. 1992. The structure of an endocytosis signal. *Trends Cell Biol.* 2:189-192.
- Vega, M. A., F. Rodriguez, B. Segui, C. Cales, J. Alcalde, and I. V. Sandoval. 1991. Targeting of lysosomal integral membrane protein LIMP II. The tyrosine-lacking carboxyl cytoplasmic tail of LIMP II is sufficient for direct targeting to lysosomes. *J. Biol. Chem.* 266:16269-16272.
- Williams, M. A., and M. Fukuda. 1990. Accumulation of lysosomal membrane glycoproteins in lysosomes requires a tyrosine residue at a particular position in the cytoplasmic tail. *J. Cell Biol.* 111:955-966.
- Yakode, M., R. K. Pathak, R. E. Hammer, M. S. Brown, J. L. Goldstein, and R. G. W. Anderson. 1992. Cytoplasmic sequence required for basolateral targeting of LDL receptor in livers of transgenic mice. *J. Cell Biol.* 117:39-46.